Dual Active Bridge based converter for integration of PV systems in the grid

Rodrigo Lopes
Instituto Superior Técnico
University of Lisbon
Lisbon, Portugal
rodrigo.abreu.lopes@tecnico.lisboa.pt

Sónia Pinto
Instituto Superior Técnico
University of Lisbon
Lisbon, Portugal
soniafp@tecnico.lisboa.pt

***Abstract* - This work aims to use a Dual Active Bridge Converter in the integration of PV panels into the grid. Currently, the need for small domestic installations of PV panels has seen an increase in demand, creating the necessity to use power converters to correctly connect them to the electrical grid. The DAB converter allows the system to meet the standards needed and operate without problems under different weather conditions. It also guarantees that the system performs at the Maximum Power Point (MPP) at any moment. It is installed alongside a DC/AC power converter to ensure the grid's connection is made smoothly and without problems.**

The simulation model presented allows the study of the converter under different temperature and irradiance conditions. It also ensures that the current injected into the grid is always sinusoidal and in phase with the grid's voltage as it should be. The model also makes it so that the system can react to a change in the weather conditions and responds accordingly, without dips or spikes.

Keywords: *Photovoltaic panel; Dual Active Bridge Converter; Maximum Power Point Tracking; Temperature; Irradiance*

I. INTRODUCTION

There has been an increase in demand for solar energy nowadays, making it an exciting new electrical energy generation option. This led to a proliferation of PV panels, both in industrial use as well as domestic use. The main differences between both uses given to PV panels are the power generated, much smaller when installed in residential areas, and being single-phase (domestic) instead of three-phase (industrial).

A PV panel is used for the conversion of solar radiation into electrical energy. This conversion is made through the photovoltaic effect, in which certain materials have the capability of producing an electric current when exposed to light [1]. Each cell of the PV panel will be composed of a P-N junction, where the electrons, excited by the photons, accelerate towards the negative terminal. Simultaneously, the positively charged holes are directed towards the positive terminal, effectively creating an electrical current.

The current and voltage generated in the PV panel will be continuous (DC) and will need to be converted into alternate (AC) to be injected into the grid. This will be the objective of the converters used. The Dual Active Bridge will be a DC/DC converter connected to an inverter (DC/AC), ensuring that the current injected into the grid meets all the norms.

A DAB converter is composed of two full-bridges composed of IGBT transistors connected by a high-frequency transformer. This transformer is used to ensure galvanic isolation and its smaller size [2] when compared to low-frequency ones. The IGBT transistors were chosen because of the switching velocity needed due to the transformer's frequency (20kHz).

The DAB converter was chosen because of its symmetric and modular structure, the bidirectional power flow capability, and the ease of soft switching [3]. Due to the bidirectionality, diodes must be placed in antiparallel with the IGBT transistors to ensure current transit in both ways.

The DAB used in this work presents a current-fed topology since it will have a low input current ripple, wide input voltage range, and high step-up ratio, making it suitable to PV applications [4].

Several modulations can be used in the DAB converter, such as Single-Phase Modulation (SPS), the Extended-Phase-Modulation (EPS), and others. The SPS was used in this work because of the ease of implementation. It is characterized by having only one phase shift between the input and output voltages and a constant duty cycle of 50% [3].

An MPPT algorithm was also implemented to ensure that the PV panel would always operate at the optimal power, no matter the weather conditions. The Incremental-Conductance algorithm was chosen because despite having the same efficiency as the P&O algorithm, it does not need to calculate the PV Power [5].

The proposed system is presented in Figure 1, where all of the previously described can be seen.

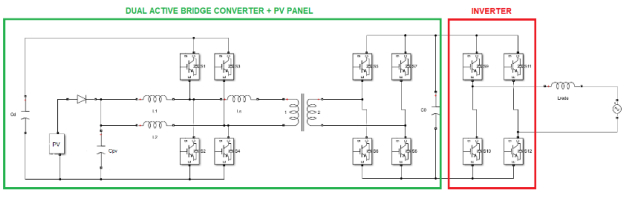

Figure 1 - Proposed System schematic

II. PROPOSED SYSTEM

A. PV Panel

The model selected in Simulink for this thesis is the Green Energy Technology GET-100A-1, arranged in 2.5 parallel strings, each with two series-connected modules. The parameters of this specific array are presented in Table 1.

Table 1 - Parameters of the PV Array

P [W]	500.9
V_{OC} [V]	192.4
V_{MP} [V]	148.4
Temperature coefficient of V_{OC} [%/ºC]	-0.39
Cells per module	106
I_{SC} [A]	4.05
I_{MP} [A]	3.375
Temperature coefficient of I_{SC} [%/ºC]	0.11

B. MPPT Algorithm

An MPPT algorithm is needed for a PV panel to be able to extract the maximum power possible. As stated before, the Inc-Cond method was chosen.

This method is based on the fact that the power slope of the PV panel at the MPP is null ($\frac{dP}{dV} = 0$). The MPP can be found in terms of the increment in the array conductance (1). This will lead to a series of conditions that express the algorithm's behavior concerning the MPP (2).

$$\frac{dP}{dV} = \frac{d(V \times I)}{dV} = I + V\frac{dI}{dV} = 0 \quad (1)$$

$$\frac{\Delta I}{\Delta V} = -\frac{I}{V} \quad (a)$$

$$\frac{\Delta I}{\Delta V} => \frac{I}{V} \quad (b)$$

$$\frac{\Delta I}{\Delta V} =< \frac{I}{V} \quad (c) \quad (2)$$

Where (a) represents the condiction at MPP, (b) represents the condiction in the left of MPP, and (c) represents the condiction in the right of MPP.

This method requires low processing since it uses only comparison, subtraction, and summation, as observed in the flowchart in Figure 2.

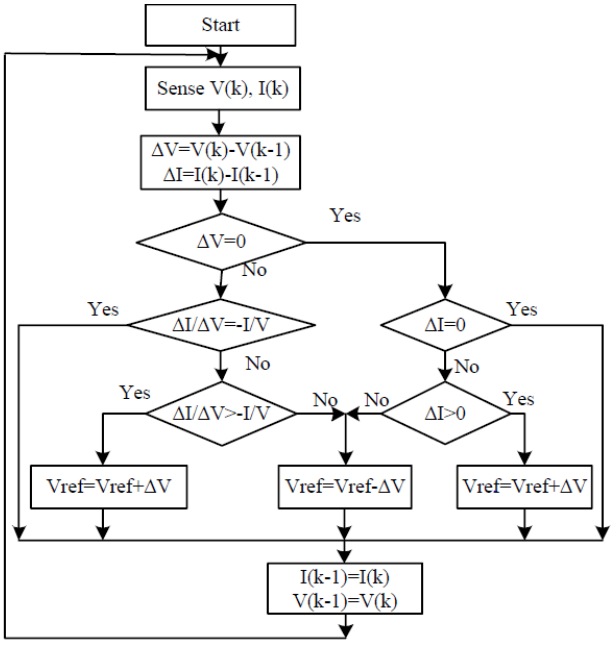

Figure 2 - DAB Flowchart

C. DAB Converter

The PV panel is connected to the DAB converter to ensure a voltage at the inverter entrance suitable to be transformed and injected into the grid. The transistors will be controlled based on the MPPT algorithm, depending on the PV panel output voltage increase or decrease.

The leakage inductor, L_S, must be sized to regulate the system's power flow since it relates the power with both the input and output voltages and the phase shift (3).

$$P = \frac{V_0 V_D}{2nf_s L_s}\frac{\varphi}{\pi}\left(1 - \frac{\varphi}{\pi}\right) \quad (3)$$

From (3), (4) can be obtained.

$$L_s = \frac{V_0 V_D}{2nf_s P}\frac{\varphi}{\pi}\left(1 - \frac{\varphi}{\pi}\right) \quad (4)$$

The output capacitor, C_0, can be sized using (5).

$$C_0 = \frac{P}{\omega_r V_0 \Delta V_0} \quad (5)$$

The input capacitor, C_d, is calculated using (6).

$$C_d = \frac{2P\Delta t}{V_{dmax}^2 - V_{dmin}^2} \quad (6)$$

In Table 2, all the relevant parameters for the sizing of the DAB converter are presented.

Table 2 - DAB Parameters

P [W]	500
V_0 [V]	593.6
V_d [V]	296.8
f_s [Hz]	20000
L_S [H]	7.05×10^{-4}
L_1 [H]	3.5×10^{-4}
L_2 [H]	3.5×10^{-4}
C_{pv} [F]	2.17×10^{-4}
C_0 [F]	4.52×10^{-4}
C_d [F]	4.22×10^{-4}

D. High-frequency Transformer

As stated before, the transformer will operate at 20kHZ. Since the output voltage will be twice the input voltage value, it will have a turns ratio of n=2, effectively making it a step-up transformer. In Table 3, the transformer parameters are shown.

Table 3 - High-frequency transformer parameters

V_{pri} [V]	296.8
V_{sec} [V]	593.6
n	2
R_m [pu]	1.25×10^{-2}
X_m [pu]	0.0083
R_P [pu]	200
X_P [pu]	33.81

E. Inverter

Having the function of injecting a sinusoidal current into the grid, the inverter will have a filtering inductor, L_r, that needs to be sized. This inductor will minimize the current ripple and the Total Harmonic Distortion (THD).

Using (7), L_r can be calculated.

$$L_r = \frac{V_0}{4 f_s \Delta i_r} \tag{7}$$

III. SYSTEM CONTROL

A. DAB Control

The control proposed for the DAB will generate and regulate two parameters, the phase shift and the duty cycle of the DAB. A two-branch control is proposed, where the first branch handles the duty cycle, and the second, the phase shift. Both will converge and be used to turn ON or OFF the transistors.

The Duty Cycle branch will have two control loops, one for the I_{pv} current and the other for the V_{pv} voltage. The Phase Shift branch will have only one loop controlling V_d. This topology is presented in Figure 3, and is based on the work done by [6].

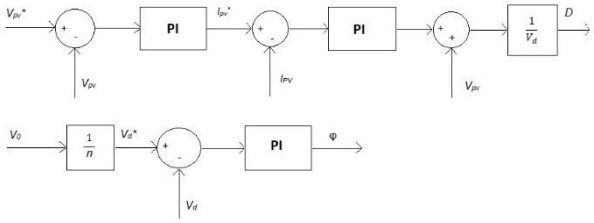

Figure 3 - DAB controller topology

As shown in Figure 3, there are four inputs to the controller, the three controlled variables, and the DAB output voltage V_0. The DAB output voltage will be controlled in the Inverter controller, but it is needed in this controller to calculate the phase shift.

Proportional-Integral (PI) compensators were used to ensure fast response velocity (proportional component) and null static error (integral component). Based on the work done by [Shi et al., 2016], it is possible to conclude that this topology will present a transfer function of fourth-order or higher in each branch, making it is a challenge to calculate the PI parameters. A different approach was used, and with the manual tuning of the PI compensators, as presented in [7], reasonable values for the PI parameters were achieved. The parameters for all the PI compensators are shown in Table 4.

Table 4 - DAB controller PI parameters

K_{pIpv}	-0.1
K_{iIPV}	-6.96
K_{pVpv}	-1
K_{iVpv}	-0.0002
K_{pVd}	-0.05
K_{iVd}	-2

B. Inverter Control

In the inverter, the grid current, I_r, and the capacitor C_0 voltage must be controlled. To control the grid current, a non-linear controller with hysteresis was used. The aim is to minimize the error, binding it inside the defined hysteresis boundaries, and follow the reference value.

Once this current control is achieved, the output voltage can be controlled. The block diagram for the output DAB voltage is shown in Figure 4.

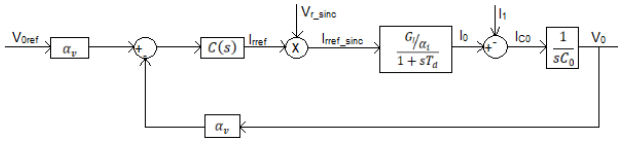

Figure 4 - Output DAB voltage controller block diagram

From Figure 4, it is possible to obtain the closed-loop transfer function of the system, presented in (8).

$$\frac{V_0(s)}{V_{0_{ref}}(s)} = \frac{\frac{\alpha_v G_i}{\alpha_i}\frac{k_{pV0}s + k_{iV0}}{C_0 T_d}}{s^3 + s^2\frac{1}{T_d} + s\frac{\alpha_v G_i}{\alpha_i}\frac{k_{pV0}}{C_0 T_d} + \frac{\alpha_v G_i}{\alpha_i}\frac{k_{iV0}}{C_0 T_d}} \tag{8}$$

Simplifying (8) and solving in order of k_{pV0} nad k_{iV0}, (9) is obtained.

$$\begin{cases} k_{pV0} = \dfrac{2.15\alpha_i C_0}{1.75^2 \alpha_v G_i T_d} \\ k_{iV0} = \dfrac{\alpha_i C_0}{1.75^3 \alpha_v G_i T_d} \end{cases} \quad (9)$$

In Table 5, all the relevant values used for the calculation of the gains are presented.

Table 5 - Inverter controller relevant parameters

α_i	1
α_v	0.01
T_d [s]	0.01
K_{pV0}	5.7910
K_{iV0}	153.9130

IV. SIMULATION RESULTS

Simulations were performed using Matlab/Simulink. The system was tested on two different situations, one where the irradiance stays constant and the temperature changes, and another one where the temperature is kept constant and the irradiance is variable.

A. *Variable Irradiance*

The irradiance will be the commanding variable in this simulation and is shown in Figure 5, where it is shown its variation. The temperature will be constant at 25ºC.

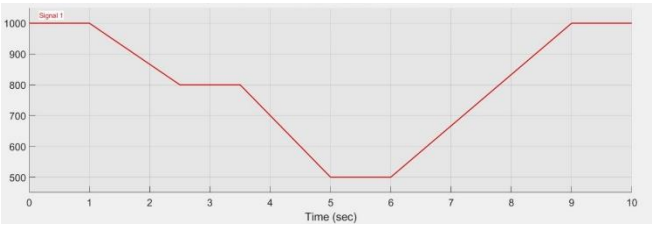

Figure 5 - Input Irradiance

The system will then calculate the reference voltage for the control of the DAB through the MPPT algorithm. The V_{ref} voltage is presented in Figure 6.

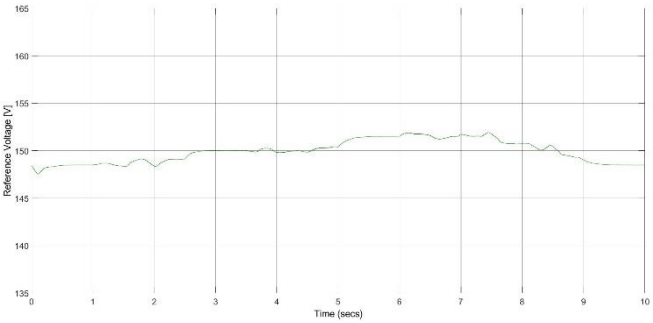

Figure 6 - Reference Voltage

Figure 7 shows all the DAB voltages are shown, such as the input voltage V_d, the output voltage V_0, and the PV panel voltage V_{pv}.

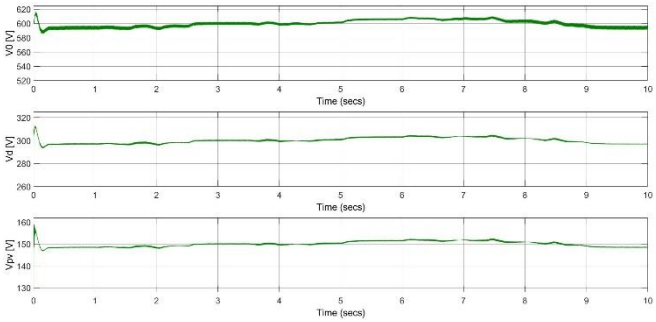

Figure 7 - DAB Voltages

It is noteworthy that in this simulation, all the parameters will have an erratic behavior in periods where the irradiance changes. It starts with the Vref voltage but will spread through the system. Despite this, it will not represent a considerable variation in the grid current due to it being attenuated in each step in the system. This behavior will have no impact on the system's power flowing, as shown in Figure 8.

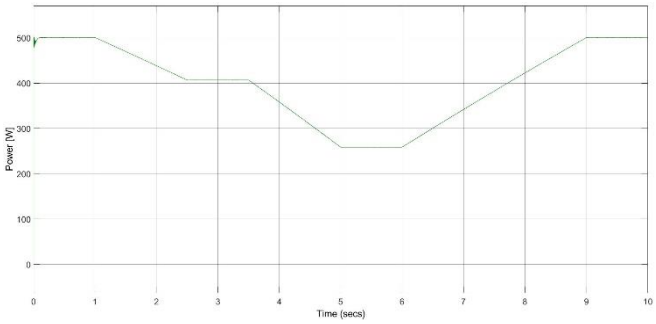

Figure 8 - DAB Power

It is also relevant to present both the duty cycle and the phase shift that the system generates while it controls itself. Since the system is operating is the SPS modulation, the duty cycle will always be 0.5, as presented in Figure 9. The phase shift will be the variable changing and controlling the currents and voltages of the DAB. It is shown in Figure 10.

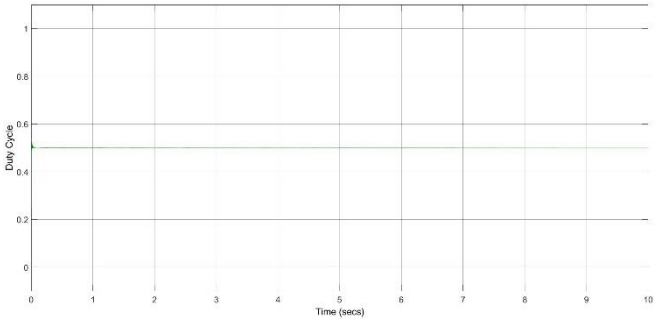

Figure 9 - Duty Cycle

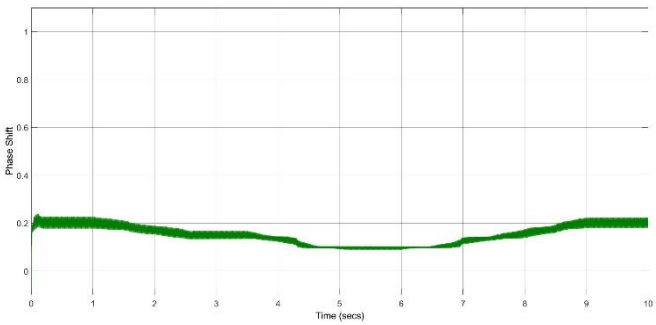

Figure 10 - Phase Shift

Finally, in Figure 11, the RMS value of the current injected into the grid is shown. The RMS value of the grid voltage, decreased by a factor of 100, is also pictured for a better understanding of the relationship between both these parameters. In Figure 12, a zoom is represented to show that both the grid current and voltage are in phase.

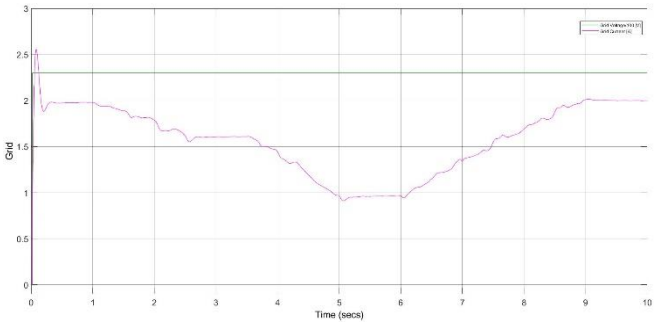

Figure 11 - Grid Voltage and Current

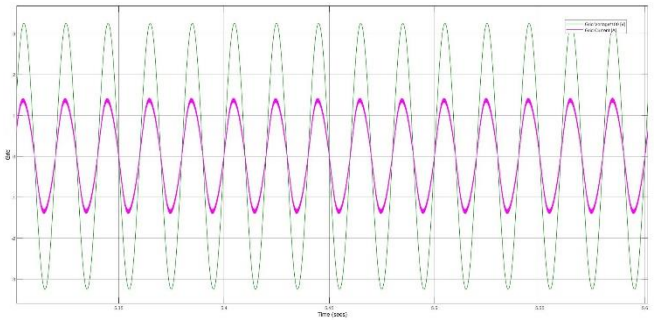

Figure 12 - Grid Voltage and Current Zoom

B. Variable Temperature

In this simulation, the temperature will be the variable changing, as represented in Figure 13. The irradiance will be constant at 1000W/m^2.

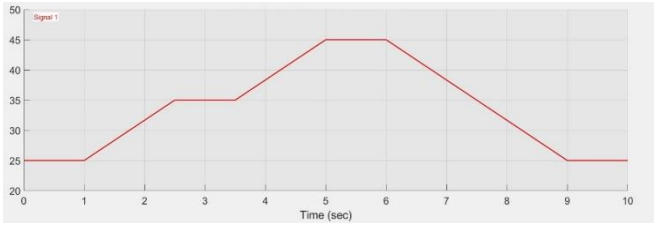

Figure 13 - Input Temperature

All of the parameters shown in the first simulation are also relevant for this one. In the first simulation, the decrease in irradiance led to an increase in the system voltages and reduced the system's currents and power. The phase shift also decreased with the imposed variation in the irradiance. In this case, it will be the opposite; the voltages will decrease, and the current, power, and phase shift, increase.

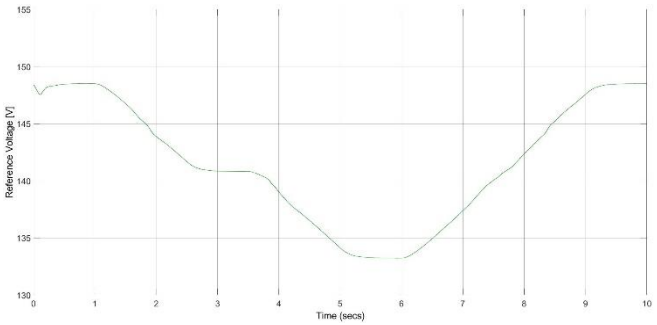

Figure 14 - Reference Voltage

Figure 14 shows the reference voltage, and Figure 15 all the voltages present in the DAB converter. As stated before, the expected decrease is verified.

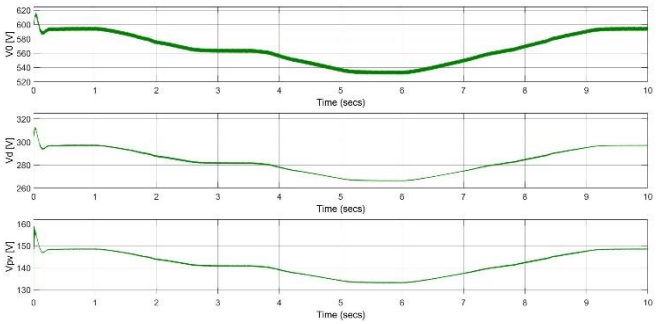

Figure 15 - DAB Voltages

It is also verified that the previous simulation's behavior is not present when the input parameter changed. This simulation will have a smoother operation and inject a current into the grid with a lower variation.

Figure 16 presents the power flowing through the system in the second simulation. It is possible to conclude that a temperature variation produces a lower variation in power than an irradiance variation.

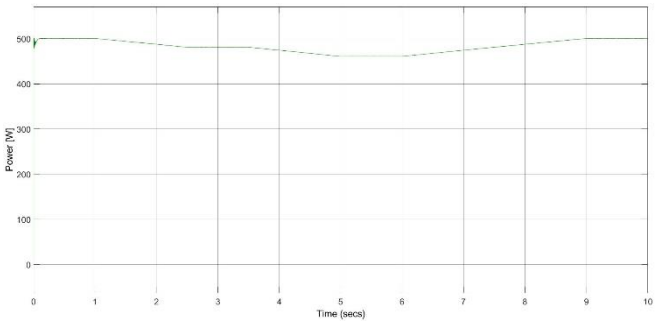

Figure 16 - DAB Power

Figure 17 and Figure 18 show the duty cycle and phase shift for this simulation. The duty cycle will once again be constant at 0.5.

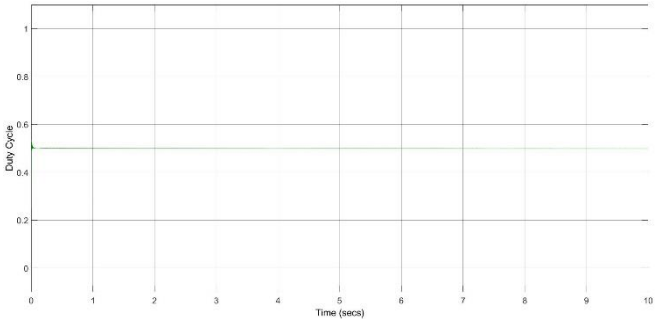

Figure 17 - Duty Cycle

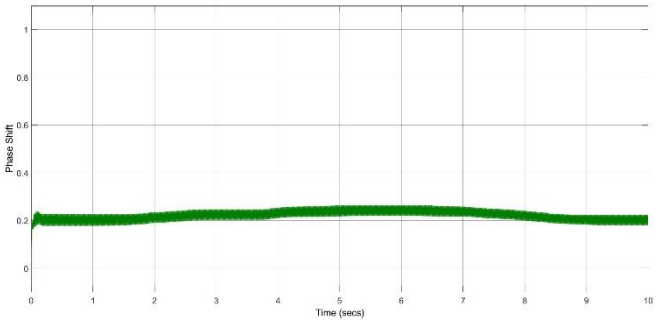

Figure 18 - Phase Shift

Lastly, the grid current and voltage RMS values are presented in Figure 19 and Figure 20. The aforementioned lower variation in the grid current can be seen in Figure 19. Figure 20 shows a zoom of both the grid parameters to show they are in phase.

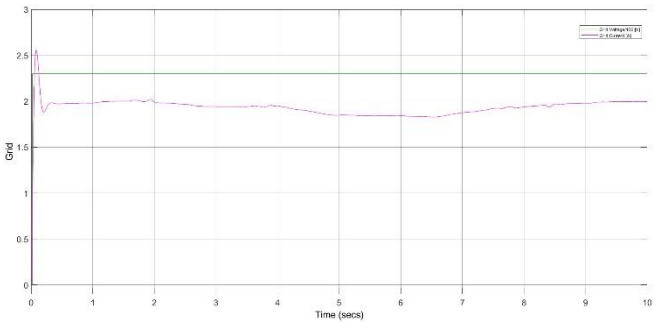

Figure 19 - Grid Voltage and Current

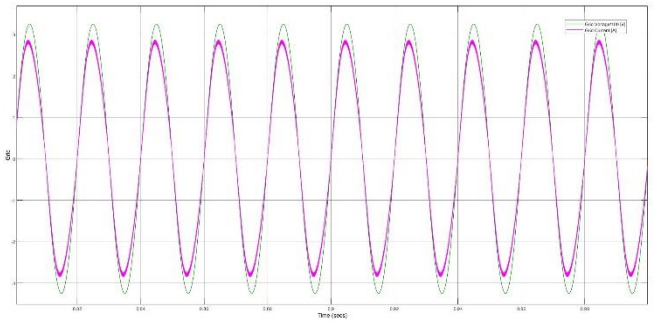

Figure 20 - Grid Voltage and Current Zoom

V. CONCLUSIONS

The proposed system consists of a photovoltaic panel connected through a DC/DC Dual Active Bridge converter and an Inverter into the grid. An MPPT algorithm was also implemented to ensure the PV panel always operates under the optimal power.

The system was simulated in Matlab/Simulink. The obtained results allow concluding that it works correctly and efficiently. Despite an unwanted variation in one of the simulations, there aren't any abrupt transitions when the system suffers changes in its inputs.

The DAB converter also has room for more complex modulations, such as the Dual-Phase-Shift (DPS) and the Triple-Phase-Shift (TPS), which will improve the results. The MPPT algorithm used can also be improved, which will lead to a stable system. Despite being a complex and arduous solution to implement, its advantages outweigh it and make it a viable solution.

REFERENCES

[1] R. Castro, **Uma Introdução às Energias Renovavéis: Eólica, Fotovoltaica e Mini-Hídrica**. 2nd Edition. Lisboa: IST Press, 2012. ISBN: 978-972-8469-01-6.

[2] W. Shen, **Design of High-density Transformers for High-frequency High-Power Converters**, Ph.D. Thesis, Virginia Polytechnic Institute, Blacksburg, Virginia, July 2006.

[3] B. Zhao, Q. Song, W. Liu, **Overview of Dual-Active-Bridge Isolated Bidirectional DC-DC Converter for High-Frequency-Link Power-Conversion System**, IEEE Transaction on Power Electronics, Vol. 29, No. 8, August 2014

[4] Y. Shi, R. Li, Y. Xue, H. Li, **Optimized Operation of Current-Fed Dual Active Bridge DC-DC Converter for PV Applications**, IEEE Transaction on Industrial Electronics, Vol. 62, No. 11, November 2015.

[5] M. A. G de Brito, L. Galotto, L. P. Sampaio, G. de A. e Melo, C. A. Canesin, **Evaluation of the Main MPPT Techniques for Photovoltaic Applications**, IEEE Transactions on Industrial Electronics, Vol. 60, No. 3, March 2013, pp 1156-1167.

[6] Y. Shi, L. Liu, Y. Xue, H. Li, **A Single-phase Grid-connected PV Converter with Minimal DC-link and Low-frequency Ripple-free Maximum Power Point Tracking**, Proc. IEEE Energy Convers. Congr. Expo, September 2013, pp 2385-2390.

[7] S. Shende, S. Pund, P. Suryawanshi, S. Potdar, **Analysis of PI Controller's Manual Tuning Technique for Residential Loads Powered by Solar Photovoltaic Arrays**, International Journal of Electrical Engineering & Technology (IJEET), Vol. 7, Issue 6, Nov-Dec 2016, pp 75-80.